*molecules*

MDPI

*Article*

# Evidence for Effective Inhibitory Actions on Hyperpolarization-Activated Cation Current Caused by *Ganoderma* Triterpenoids, the Main Active Constitutents of *Ganoderma* Spores

**Wei-Ting Chang [1,2,3], Zi-Han Gao [4], Yi-Ching Lo [5] and Sheng-Nan Wu [4,6,7,*]**

1 Division of Cardiovascular Medicine, Chi-Mei Medical Center, Tainan 71004, Taiwan; cmcvecho2@gmail.com
2 Department of Biotechnology, Southern Taiwan University of Science and Technology, Tainan 71004, Taiwan
3 Institute of Clinical Medicine, College of Medicine, National Cheng Kung University, Tainan 70101, Taiwan
4 Department of Physiology, National Cheng Kung University Medical College, Tainan 70101, Taiwan; hhelen000111tw@gmail.com
5 Department of Pharmacology, College of Medicine, Kaohsiung Medical University, Kaohsiung 80708, Taiwan; yichlo@kmu.edu.tw
6 Institute of Basic Medical Sciences, National Cheng Kung University Medical College, Tainan 70101, Taiwan
7 Department of Medical Research, China Medical University Hospital, China Medical University, Taichung 40402, Taiwan
* Correspondence: snwu@mail.ncku.edu.tw; Tel.: +88-662-353-535-5334; Fax: +88-662-362-780

Received: 7 October 2019; Accepted: 20 November 2019; Published: 22 November 2019


**Abstract:** The triterpenoid fraction of *Ganoderma* (*Ganoderma* triterpenoids, GTs) has been increasingly demonstrated to provide effective antioxidant, neuroprotective or cardioprotective activities. However, whether GTs is capable of perturbing the transmembrane ionic currents existing in electrically excitable cells is not thoroughly investigated. In this study, an attempt was made to study whether GTs could modify hyperpolarization-activated cation currents ($I_h$) in pituitary tumor ($GH_3$) cells and in HL-1 atrial cardiomyocytes. In whole-cell current recordings, the addition of GTs produced a dose-dependent reduction in the amplitude of $I_h$ in $GH_3$ cells with an $IC_{50}$ value of 11.7 μg/mL, in combination with a lengthening in activation time constant of the current. GTs (10 μg/mL) also caused a conceivable shift in the steady-state activation curve of $I_h$ along the voltage axis to a more negative potential by approximately 11 mV. Subsequent addition of neither 8-cyclopentyl-1,3-dipropylxanthine nor 8-(*p*-sulfophenyl)theophylline, still in the presence of GTs, could attenuate GTs-mediated inhibition of $I_h$. In current-clamp voltage recordings, GTs diminished the firing frequency of spontaneous action potentials in $GH_3$ cells, and it also decreased the amplitude of sag potential in response to hyperpolarizing current stimuli. In murine HL-1 cardiomyocytes, the GTs addition also suppressed the amplitude of $I_h$ effectively. In DPCPX (1 μM)-treated HL-1 cells, the inhibitory effect of GTs on $I_h$ remained efficacious. Collectively, the inhibition of $I_h$ caused by GTs is independent of its possible binding to adenosine receptors and it might have profound influence in electrical behaviors of different types of electrically excitable cells (e.g., pituitary and heart cells) if similar in vitro or in vivo findings occur.

**Keywords:** *Ganoderma* triterpenoids; hyperpolarization-activated cation current; current kinetics; membrane potential; pituitary cell; heart cell

## 1. Introduction

*Ganoderma* mushrooms (Língzhī in Chinese, or Reishi in Japanese) are a traditional Chinese herbal medicine that has been widely accepted as a nutritional supplement. Among many species of the

mushrooms, *Gandoderm lucidum* (GL) is most commonly seen and is commercially cultivated under controlled conditions to obtain mushrooms with more consistent chemical composition [1]. GL was reported to possess a variety of biological activities for its medicinal use, such as antihypertensive, hypoglycemic and hypocholesterolemic activities among other medicinal benefits [1–4]. The primary bioactive compounds in GL were noted to include triterpenoids [4–7]. GL was also shown to prevent cardiac damage in animal models by alleviating the oxidative stress associated with myocardial injury [8].

Triterpenes are a subclass of terpenes and have a basic skeleton of $C_{30}$. Triterpenoids have molecular weights ranging from 400 to 600 kDa, and their chemical structure is complex and noted to be highly oxidized [9]. The triterpenoid fraction of *Ganoderma*, consisting of more than 300 lanostane-tetracyclic compounds, has been growingly demonstrated to be effective at exerting an array of biological actions such as that known either to provide effective antioxidant activities for prevention of myocardial injury, or to produce neuroprotective actions [2–6,10–21]. *Ganoderma* triterpenoids (GTs) could also suppress inflammatory response by directly scavenging the free radicals or systemically enhancing the antioxidant enzymes, thereby lowering lipid peroxidase in chicken livers or mice [2,3,8,17,20–23]. The aqueous extract from GL was previously reported to exert anti-convulsant, anti-depressive, anxiolytic and anti-nociceptive actions [6,12,24,25]. However, whether GTs produces any perturbations on membrane ionic currents or membrane potential in electrically excitable cells (e.g., endocrine or heart cells) is not thoroughly studied.

Hyperpolarization-activated cation current ($I_h$) has been well recognized as a key determinant of repetitive electrical activity in heart cells and in an array of sensory or central neurons, and neuroendocrine or endocrine cells [26–35]. This current is a mixed inward $Na^+/K^+$ current, which is sensitive to block by CsCl, ivabradine or zatebradine [29,36,37], and the rise in this current can consequently act to depolarize membrane potential to threshold required for the generation of action potential (AP) [28,30,31,33]. The $I_h$ was demonstrated to be carried by channels of the hyperpolarization-activated cyclic nucleotide-gated (HCN) gene family, which belongs to the superfamily of voltage-gated $K^+$ channels and cyclic nucleotide-gated channels. However, how or whether GTs is capable of interacting with HCN channels to modify the amplitude and gating of $I_h$ is largely unknown.

Therefore, the objective of this work was to test whether GTs could exert any modifications on ionic currents (e.g., $I_h$) present in pituitary $GH_3$ cells and HL-1 cardiomyocytes. The biophysical and pharmacological properties of ionic currents, in particular $I_h$ in these cells, were extensively characterized. Current-clamp voltage recordings were also made to evaluate whether GTs could perturb spontaneous action potentials and sag potentials present in $GH_3$ cells. Findings from the present results highlight the notion that GTs can modify the amplitude and gating of $I_h$ in a concentration-, time- and state-dependent manner.

## 2. Results and Discussion

### *2.1. Inhibitory Effect of GTs on Hyperpolarization-Activated Cation Current ($I_h$) Recorded from Pituitary $GH_3$ Cells*

In an initial stage of whole-cell experiments designed for the recording of $I_h$, we bathed cells in $Ca^{2+}$-free, Tyrode's solution and, during the measurements, we filled the pipette by using a $K^+$-containing solution. The reason why we used $Ca^{2+}$-free, Tyrode's solution is to eliminate contamination of $Ca^{2+}$-activated $K^+$ currents that could be possibly generated by any activity of small- or intermediate-conductance $Ca^{2+}$-activated $K^+$ channels. As shown in Figure 1A, the $I_h$, which was identified and then characterized by the slowly activating property [27,29,38], could be readily evoked by membrane hyperpolarization to −122 mV with a duration of 2 sec. As the cells were exposed to different concentrations of GTs, the $I_h$ amplitude was progressively decreased and the activating time course of the current also concomitantly became slowed. For example, the addition of 30 μg/mL GTs decreased $I_h$ amplitude from 621 ± 23 to 295 ± 13 pA ($n = 8$, $p < 0.05$). In combination with these results,

the value of activation time constant ($\tau_{act}$) of $I_h$ elicited by 2-sec maintained hyperpolarization was also raised to 680 ± 25 msec ($n$ = 8, $p < 0.05$) from a control value (i.e., in the absence of GTs) of 467 ± 21 msec ($n$ = 8). After washout of GTs, the current amplitude was returned to 609 ± 18 pA ($n$ = 7, $p < 0.05$). The dose-dependent relationship of inhibitory effect of GTs is illustrated in Figure 1B. The $IC_{50}$ value required for GTs-mediated inhibition of $I_h$ amplitude taken at the end of hyperpolarizing pulse was then constructed with a modified Hill equation (as detailed in Materials and Methods) and calculated to be 11.7 μM with a Hill coefficient of 1.2, and this agent at a dose of 100 μg/mL nearly abolished the $I_h$ amplitude.

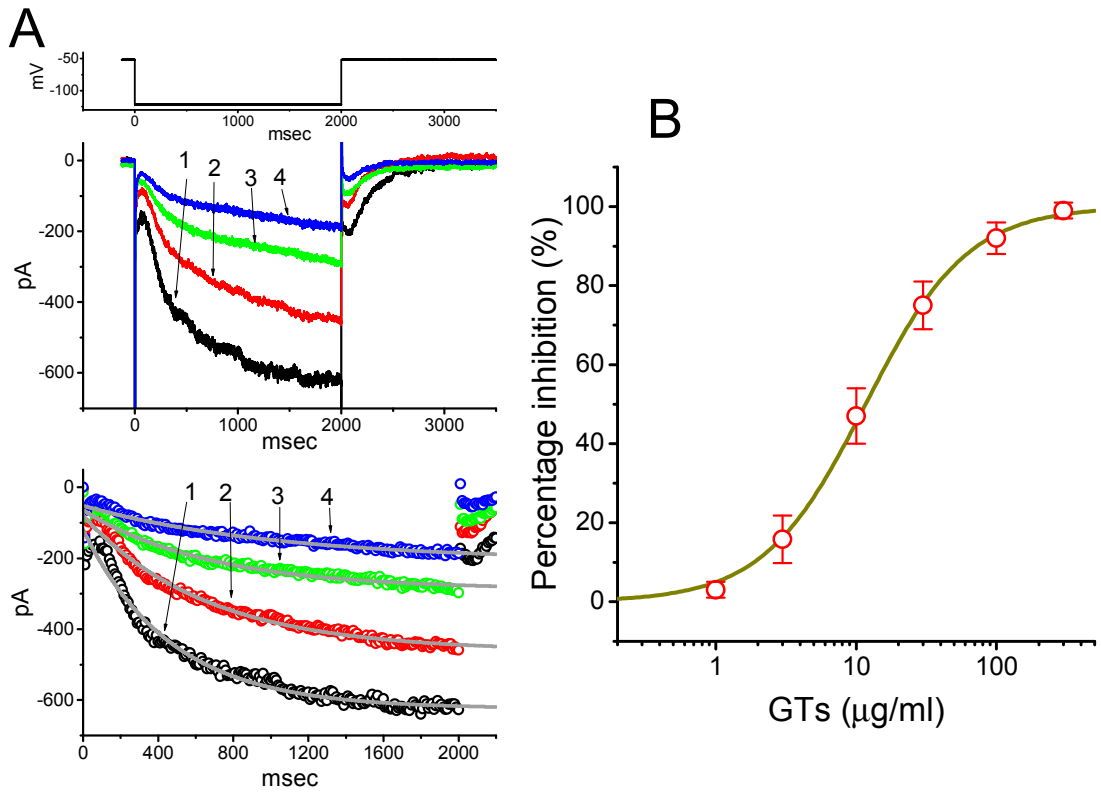


**Figure 1.** Effect of *Ganoderma* triterpenoids (GTs) on hyperpolarization-activated cation current in pituitary tumor ($GH_3$) cells. In these whole-cell current recordings, cells were bathed in $Ca^{2+}$-free, Tyrode's solution, and we backfilled the recording electrode by using a $K^+$-containing solution. The hyperpolarizing step from −52 to −122 mV was applied to the examined cells. (**A**) Superimposed $I_h$ traces obtained in the absence (1) and presence of 10 μg/mL GTs (2), 30 μg/mL GTs (3) and 100 μg/mL GTs (4). The uppermost part is the voltage profile used. The lower part depicts the trajectory of each $I_h$ trace shown in the upper panel (in the absence (1) and presence of 10 μg/mL GTs (2), 30 μg/mL GTs (3) and 100 μg/mL GTs (4)) was fitted by single exponential with the activation time constant ($\tau_{act}$) of 467, 657, 680 and 1037 msec, respectively. For better illustration, the data points (circles symbols) were reduced by a factor of 10. (**B**) Dose-dependent relation of GTs effect on $I_h$ amplitude (mean ± SEM; n = 7–9 for each point). The $I_h$ amplitudes were taken at the end of 2-sec hyperpolarizing step in the presence of different GTs doses. The continuous line was fitted with the goodness of fit by a modified Hill function described under Materials and Methods. The $IC_{50}$ value required for GTs-induced suppression of $I_h$ was computed to be 11.7 μg/mL.

### 2.2. *Effect of GTs on the Averaged I–V Relationship of $I_h$ Recorded from $GH_3$ Cells*

We further tested whether the presence of GTs could exert any perturbations on the *I–V* relationship of $I_h$ in these cells. As illustrated in Figure 2, the $I_h$ traces were evoked by a series of voltage pulses ranging from −132 to −52 mV in 10-mV increments. Within 2 min of exposing cells to 10 μg/mL GTs, the amplitudes of $I_h$ examined throughout the entire voltage-clamp steps (e.g., an inwardly rectifying

property) were significantly decreased. For example, at the level of −132 mV, the addition of 10 μg/mL GTs reduced current amplitude from 261.5 ± 23 to 132.6 ± 14 pA ($n$ = 8, $p < 0.05$). Likewise, in the presence of 10 μg/mL GTs, the whole-cell $I_h$ conductance measured at the voltage ranging between −102 and −132 mV was decreased by 43% ± 2% to 3.67 ± 0.12 nS ($n$ = 8, $p < 0.05$) from a control value of 6.48 ± 0.21 nS ($n$ = 8).

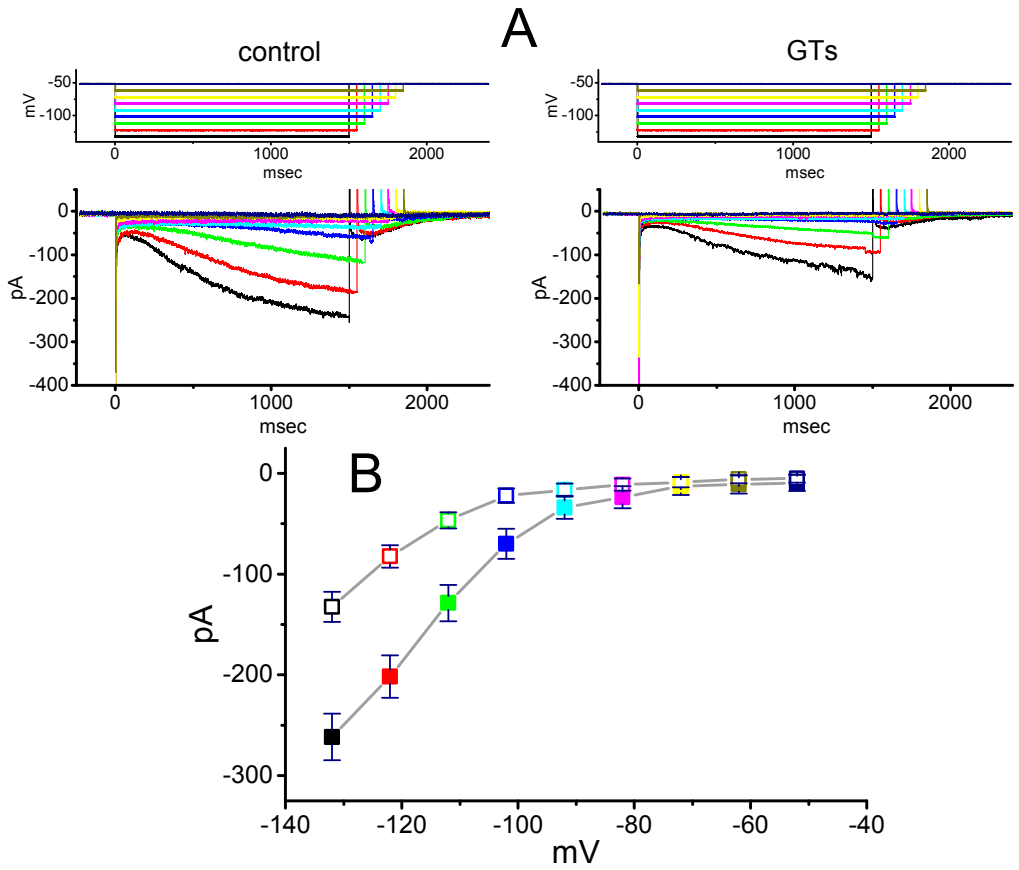


**Figure 2.** Effect of GTs on average current–voltage ($I$–$V$) relationship of $I_h$ recorded from $GH_3$ cells. The examined cell was maintained at −52 mV and a series of voltage steps ranging from −132 to −52 mV from a holding potential of −52 mV in 10-mV increments was thereafter applied. (**A**) Superimposed $I_h$ traces in the absence (left, control) and presence (right) of 10 μg/mL GTs. The upper part in each panel indicates the voltage protocol used. Notably, during our voltage-clamp recordings, colored labeling in each current trace (lower part) in the absence (left) and presence (right) of GTs corresponds to that in voltage trace (upper part). (**B**) Averaged $I$–$V$ relationships of $I_h$ amplitude with or without the GTs addition (mean ± SEM; $n$ = 8 for each point). The examined cells were voltage-clamped at −52 mV, current amplitude was then taken at the end of each hyperpolarizing step, and colored labeling in each point corresponds to that in (**A**). Closed symbols: control; Open symbols: in the presence of 10 μg/mL GTs.

### 2.3. Modification of the Steady-State Activation Curve of $I_h$ Produced by the Presence of GTs

To characterize the inhibitory effect of GTs on $I_h$ in $GH_3$ cells, we further investigated its possible modifications on the steady-state activation curve of $I_h$. Figure 3 illustrates the steady-state activation curve of $I_h$ obtained with or without addition of GTs (10 μg/mL). A two-step voltage pulse protocol created through digital-to-analog conversion was applied in this set of experiments. That is, a 2-sec conditioning pulse to various membrane potentials preceded the test pulse (2 sec in duration) to −122 mV from a holding potential of −52 mV. During the measurements, the intervals between two sets of voltage pulses were about 2 min to allow complete recovery of $I_h$. The relationships between the conditioning potentials and the normalized amplitudes ($I/I_{max}$) of $I_h$ in the absence and presence of

10 μg/mL GTs were then constructed and fitted to a Boltzmann function as described under Materials and Methods. In control, $V_{1/2}$ = −86.3 ± 7.1 mV, $q$ = 1.81 ± 0.04 $e$ ($n$ = 9), whereas during cell exposure to 10 μg/mL GTs, $V_{1/2}$ = −107.3 ± 6.9 mV, $q$ = 1.84 ± 0.04 $e$ ($n$ = 9). It appeared, therefore, that the presence of GTs not only decreased the maximal conductance of $I_h$, but also significantly shifted the activation curve along the voltage axis to a hyperpolarized potential by approximately 11 mV. However, we were unable to find significant change in the gating charge of the curve taken between the absence and presence of 10 μg/mL GTs. This occurrence indicates that the addition of GTs is capable of altering the steady-state activation curve of $I_h$.

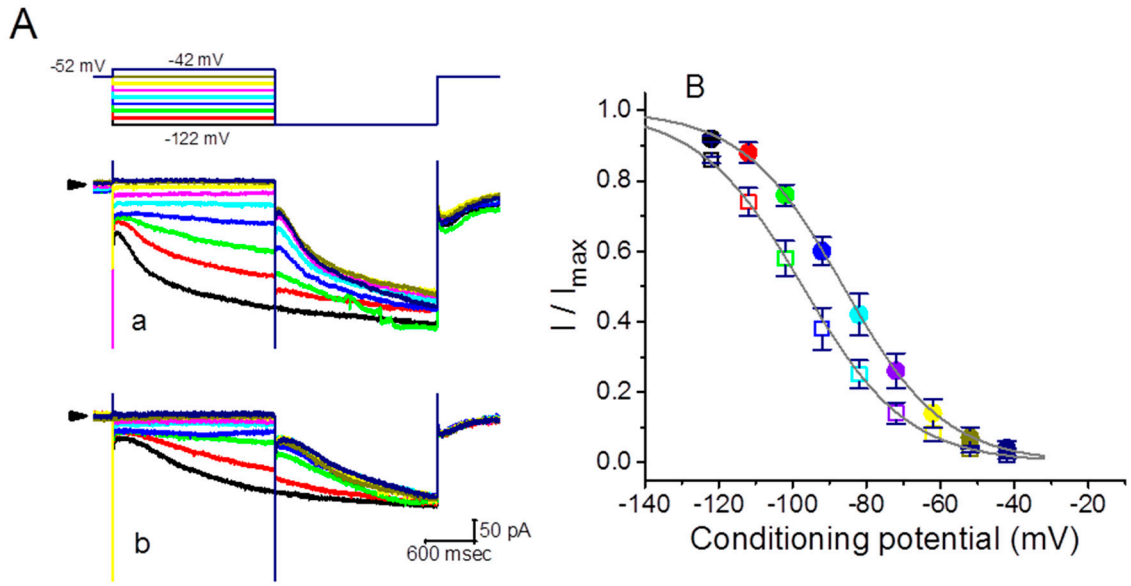


**Figure 3.** Effect of GTs on the steady-state activation curve of $I_h$ measured from $GH_3$ cells. The recording experiments were conducted in a two-step voltage pulse. The conditioning voltage pulses with a duration of 2 sec to potentials ranging from −122 and −42 mV. After each conditioning pulse, a test pulse to −122 mV with a duration of 2 sec was applied to evoke $I_h$. (**A**) Representative $I_h$ traces evoked by this two-step protocol. Current traces labeled a are the control, and those labeled b were obtained in the presence of 10 μg/mL GTS. The uppermost part is the voltage protocol applied, arrowhead in the left side of each panel denotes the zero current level, and calibration mark at the right lower corner applies all current traces in (**A**). Notably, colored labeling in each current trace (lower part) in the absence (a) and presence (b) of GTs corresponds to that in voltage trace (upper part). (**B**) Steady-state activation curves of $I_h$ obtained in the absence (closed symbols) and presence (open symbols) of 10 μg/mL GTs (mean ± SEM, $n$ = 9 for each point). Current amplitude was taken at the end of hyperpolarizing pulse. The sigmoidal smooth lines indicate the least-squares fit to the Boltzmann equation detailed in Materials and Methods. Colored labeling in each point corresponds to that in (**A**).

### *2.4. Comparisons Among the Effects of GTs, GTs Plus 8-Cyclopentyl-1,3-dipropylxanthine (DPCPX), GTs Plus 8-(p-Sulfophenyl)theophylline (8-PST), GTs Plus Oxaliplatin (OXAL) and GTs Plus Carboxiplatin (Carb) in $I_h$ Amplitude*

In the next set of experiments, we further investigated whether subsequent addition of DPCPX, 8-PST, oxaliplatin or carboxiplatin, but still in continued presence of GTs, was able to modify GTs-mediated inhibition of $I_h$ inherently in $GH_3$ cells. As shown in Figure 4, further application of neither DPCPX (1 μM) nor 8-PST (10 μM) effectively perturbed the inhibition of $I_h$ produced by 10 μg/mL GTs, despite the ability of GTs to suppress $I_h$ amplitude together with the slowing in current activation. DPCPX or 8-PST was reported to be antagonist of adenosine $A_1$ receptors [39]. However, in continued presence of 10 μg/mL GTs, further addition of oxaliplatin (10 μM) or carboxiplatin (10 μM) was able to reverse GTs-mediated effectiveness in the suppression of $I_h$. Oxaliplatin was recently reported to activate HCN-encoded current [40].

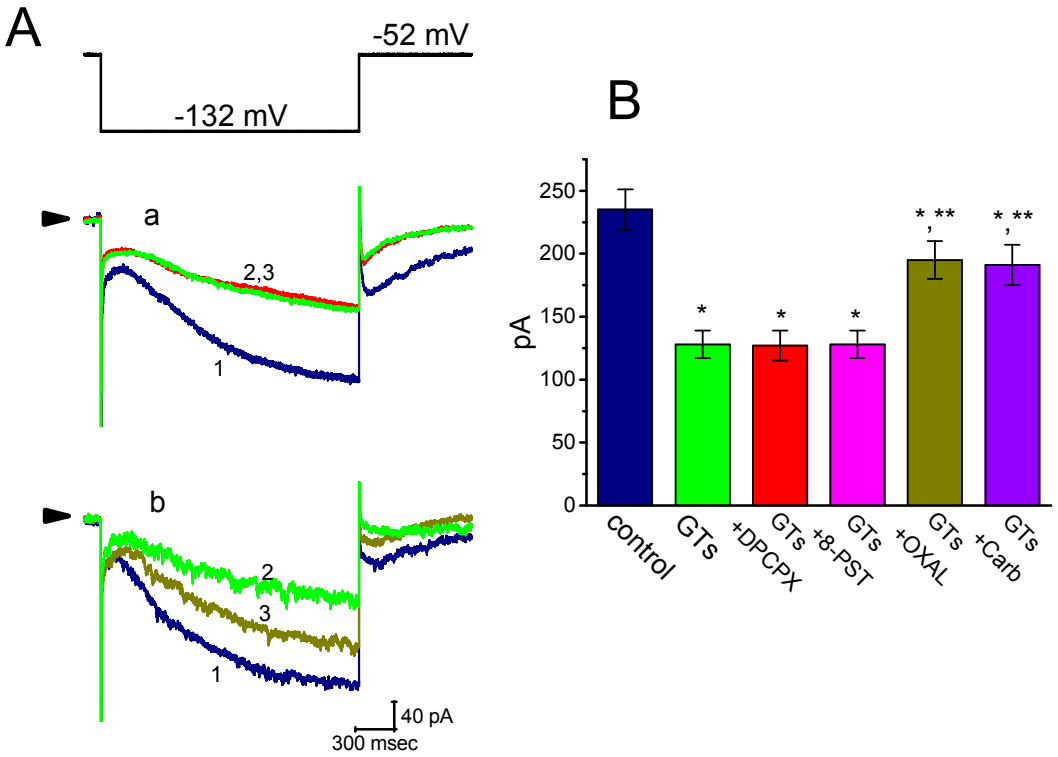


**Figure 4.** Comparisons among the effects of GTs, GTs plus 8-cyclopentyl-1,3-dipropylxanthine (DPCPX), GTs plus 8-(*p*-sulfophenyl)theophylline (8-PST), GTs plus oxaliplatin (OXAL) and GTs plus carboxiplatin (Carb) on $I_h$ amplitude in $GH_3$ cells. Current amplitude was taken at the end of 2-sec hyperpolarizing pulse to −122 mV. (**A**) Superimposed $I_h$ traces elicited in response to step hyperpolarization (as indicated in the uppermost part). In panels a and b, current traces labeled 1 are controls and those labeled 2 were obtained in the presence of 10 μg/mL GTs alone, while in panel a or b that labeled 3 was, respectively, taken in the addition of 1 μM DPCPX (a) or 10 μM oxaliplatin (b), but still in continued presence of 10 μg/mL GTs. Arrows in current traces of each panel indicate the zero current level, and calibration mark shown in the right lower corner applies all current traces. (**B**) Summary bar graph showing the effects of GTs (10 μg/mL), GTs plus DPCPX (1 μM), GTs plus 8-PST (10 μM), GTs plus oxaliplatin (10 μM) and GTs plus carboxiplatin (10 μM) on $I_h$ amplitude measured from $GH_3$ cells (mean ± SEM; $n$ = 6–9 for each bar). Current amplitude was obtained at the end of hyperpolarized pulse from −52 to −122 mV. DPCPX: 1 μM 8-cyclopentyl-1,3-dipropylxanthine; 8-PST: 10 μM 8-(*p*-sulfophenyl)theophylline; OXAL: 10 μM oxaliplatin; Carb: 10 μM carboxiplatin. *Significantly different from control ($p < 0.05$) and **significantly different from 10 μg/mL alone group ($p < 0.05$).

### 2.5. *Effects of GTs on the Firing of Spontaneous Action Potentials (APs) Recorded from $GH_3$ Cells*

In another set of experiments, we further tested whether GTs produces any effectiveness in spontaneous APs inherently in $GH_3$ cells [31,38,41]. Cells were immersed in normal Tyrode's solution containing 1.8 mM $CaCl_2$ and current-clamp voltage recordings were performed to measure the occurrence of spontaneous APs. Of note, as cells were exposed to GTs, the firing of spontaneous APs was progressively decreased (Figure 5). Within 2 min of exposing cells to 10 μg/mL GTs, the resting potential was shifted to the hyperpolarized direction, in combination with the decreased frequency of spontaneous APs and with appearance of depressed pacemaker potential. Similarly, the addition of zatebradine (10 μM), an inhibitor of $I_h$ [36,42], was also found to depress the firing frequency of APs significantly. Therefore, changes in the frequency of spontaneous APs produced by either GTs or zatebradine could conceivably be linked to a mechanism via the inhibition of $I_h$ described above.

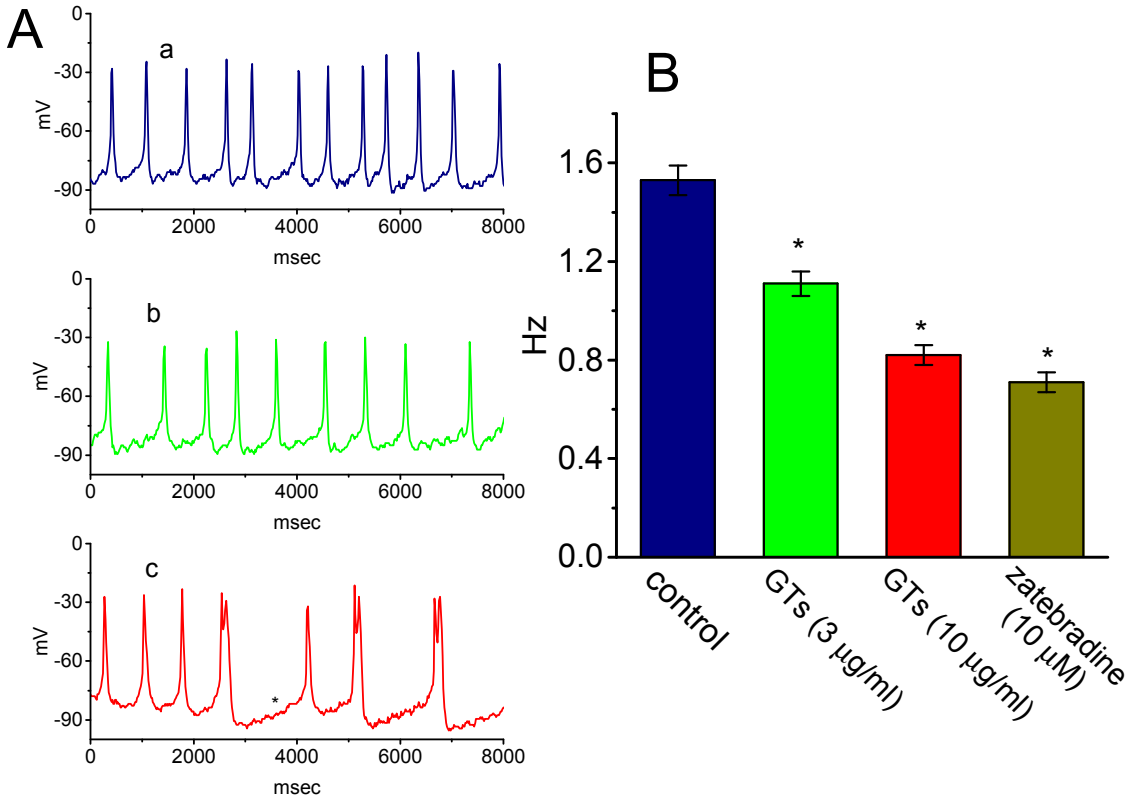


**Figure 5.** Effect of GTs on the firing of spontaneous action potentials (APs) in $GH_3$ cells. Cells were bathed in normal Tyrode's solution containing 1.8 mM $CaCl_2$, the pipette used was filled with $K^+$-containing solution, and current-clamp voltage recordings were made. (**A**) Potential trace obtained in the absence (a) and presence of 3 μg/mL GTs (b) or 10 μg/mL GTs (c). The asterisk in potential trace labeled c indicates the depressed pacemaker potential. (**B**) Summary bar graph showing the effects of GTs and zatebradine (10 μM) on the firing frequency of spontaneous APs (mean ± SEM; $n = 8$ for each bar). *Significantly different from control ($p < 0.05$).

### *2.6. Effect of GTs on Sag Potential in $GH_3$ Cells*

Another set of current-clamp recordings was next made in attempts to evaluate the possible presence of sag potential, which is closely linked to the emergence of $I_h$ [43]. As shown in Figure 6, under our experimental condition, when the whole-cell voltage recordings were firmly established, hyperpolarizing current injection with the amplitude of around 25 pA was found to induce sag potential (i.e., drop down to a lower level in the membrane potential upon hyperpolarizing current stimuli). The addition of zatebradine or GTs was effective at decreasing the amplitude of sag potential, while chlorotoxin (1 μM) was unable to modify sag potential in these cells. For example, cell exposure to GTs (10 μg/mL) decreased the amplitude from 48 ± 9 to 22 ± 5 mV ($n = 7$, $p < 0.05$). Moreover, subsequent application of oxaliplatin (10 μM), still in the presence of GTs (10 μg/mL), attenuated GTs-induced suppression of sag potential, as evidenced by a significant increase of sag potential to 39 ± 8 mV ($n = 7$, $p < 0.05$). However, chlorotoxin (1 μM) alone, a blocker of $Cl^-$ channels, did not produce any effect on sag potential in these cells (data not shown). Therefore, the depression of sag potential caused by GTs could result largely from its inhibitory effect on $I_h$ observed in $GH_3$ cells.

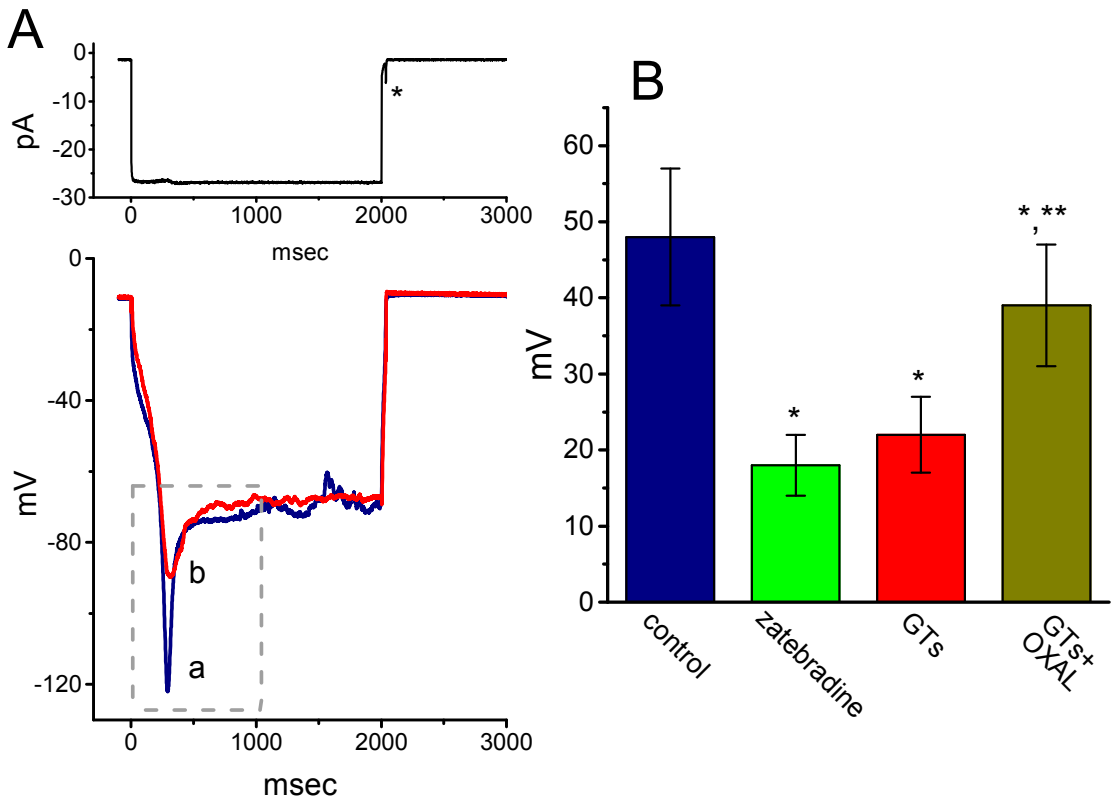


**Figure 6.** Effect of GTs on sag potential recorded under the current-clamp configuration in $GH_3$ cells. Cells were bathed in normal Tyrode's solution and we filled the recording pipette with $K^+$-containing solution. As the whole-cell recordings were established, the experiment was swiftly switched to current-clamp condition with 2-sec hyperpolarizing current stimuli. (**A**) Potential traces obtained in the absence (a) and presence (b) of 10 μg/mL GTs. Dashed box indicates the sag potential in response to long-lasting hyperpolarizing current (as indicated in the upper part), and the asterisk is the action current taken as membrane potential return to the resting potential. (**B**) Summary bar graph showing the effects of zatebradine (10 μM), GTs (10 μg/mL) and GTs (10 μg/mL) plus oxaliplatin (OXAL, 10 μM) on the amplitude of sag potential in $GH_3$ cells (mean ± SEM; $n = 7$ for each bar). *Significantly different from control ($p < 0.05$) and **significantly different from GTs alone group ($p < 0.05$).

### 2.7. *Effect of GTs on $I_h$ Recorded from HL-1 Cardiomyocytes*

It has been shown that GL might prevent cardiac damage by decreasing the oxidative stress associated with myocardial injury [8]. We therefore also tested whether GTs exerts any effects on $I_h$ present in HL-1 heart cells [44,45]. These experiments were conducted in cells bathed in $Ca^{2+}$-free Tyrode's solution, and the downsloping ramp pulse from −52 to −162 mV with a duration of 1 sec was applied to evoke $I_h$ in these cells. As shown in Figure 7, the $I_h$ evoked by such long-lasting ramp pulse was subject to be suppressed by the addition of GTs. For example, as the cells were exposed to 10 μg/mL GTs, current amplitude measured at the level of −152 mV was profoundly decreased to 193 ± 14 pA ($n = 8$, $p < 0.05$) from a control level of 369 ± 23 pA ($n = 8$). Likewise, under such a downsloping ramp pulse, the presence of 10 μg/mL GTs profoundly decreased the whole-cell $I_h$ conductance measured ranging between −152 and −132 mV from 7.72 ± 0.16 to 4.2 ± 0.12 nS ($n = 8$, $p < 0.05$). Moreover, the addition of 10 μM oxaliplatin, still in the presence of 10 μg/mL GTs, attenuated current amplitude suppressed by GTs, as evidenced by a significant increase in $I_h$ amplitude to 278 ± 19 pS ($n = 8$, $p < 0.05$). In DPCPX-treated HL-1 cells, GTs-mediated inhibition of $I_h$ remained unchanged (data not shown). Therefore, consistent with the observations made above in $GH_3$ cells, the GTs addition effectively inhibited the amplitude of $I_h$ in response to long-lasting membrane hyperpolarization in HL-1 cardiomyocytes.

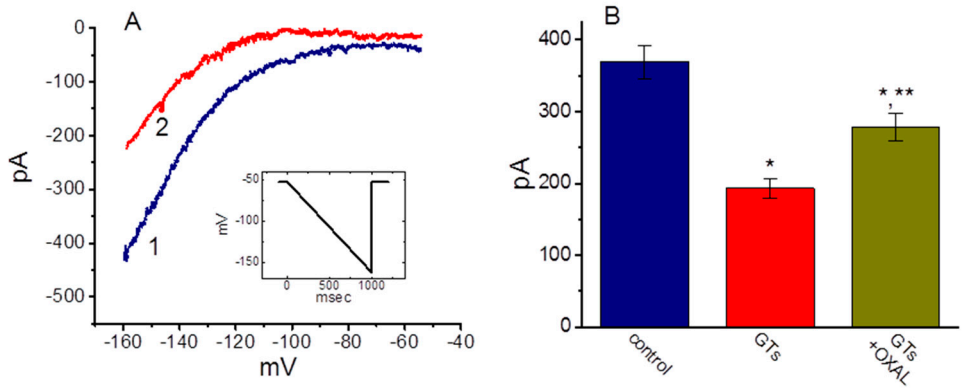


**Figure 7.** Effect of GTs on $I_h$ elicited by a downsloping ramp pulse in HL-1 cardiomyocytes. In these experiments, the examined cell was maintained at −52 mV and the linear ramp pulse from −52 to −162 mV with a duration of 1 sec (as indicated in inset of (**A**)). (**A**) Representative $I_h$ traces in response to such linear ramp obtained with or without the addition of GTs. Current trace labeled 1 is control, and that labeled 2 was obtained 2 min after addition of 10 μg/mL GTs. (**B**) Summary bar graph showing effect of GTs and GTs plus oxaliplatin on $I_h$ elicited by ramp pulse. Current amplitude was measured at the level of −152 mV. Each bar indicates the mean ± SEM ($n$ = 7–8). * Significantly different control ($p < 0.05$) and ** significantly different from 10 μg/mL GTs alone group ($p < 0.05$).

The present results demonstrated that the inhibition by GTs of $I_h$ in $GH_3$ cells did not simply decrease current magnitude but also altered the kinetics of the current, thereby indicating that it is able to produce a dose-, time- and state-dependent activation of $I_h$. The steady-state activation curve of $I_h$ in the presence of GTs was shifted along voltage axis toward the less depolarized potential. The $IC_{50}$ value (i.e., 11.7 μg/mL) required for GTs-mediated inhibition of $I_h$ observed in $GH_3$ cells is similar to that used for anti-oxidative or neuroprotective properties [2–4,15–17,46,47]. Such intriguing actions could be of pharmacological relevance and appear to be upstream of its effects on oxidative stress occurring inside the cell.

Previous works have demonstrated that GTs could abundantly contain various nucleosides including adenosine [48–50]. Adenosine has been previously reported to modify the amplitude of $I_h$ in heart cells (i.e., sinoatrial cells) [26,51]. However, further application of neither DPCPX nor 8-PST, still in the presence of GTs, was capable of attenuating GTs-mediated inhibition of $I_h$ effectively. DPCPX or 8-PST was previously reported to be blocker of adenosine $A_1$ receptor [39]. Moreover, subsequent addition of oxaliplatin or carboxiplatin, in continued presence of GTs, significantly reversed the $I_h$ amplitude suppressed by GTs. Oxaliplatin was recently found to activate HCN-encoded current [40]. Subsequent addition of adenosine deaminase (2 unit/mL), in continued presence of GTs, did not modify GTs-mediated inhibition of $I_h$ in $GH_3$ cells (data not shown). Consequently, it seems unlikely that GTs-mediated block of $I_h$ observed in $GH_3$ cells ascribes predominantly from nucleosides (e.g., adenosine) possibly contained in the ingredients of GTs.

Previous studies have demonstrated the ability of GTs to have an inhibitory effect on the activity of acetylcholinesterase [4,47]. However, we were unable to find that further application of atropine (10 μM), an antagonist of muscarinic receptors, could modify GTs-mediated suppression of $I_h$ in $GH_3$ or HL-1 cells (data not shown). It seems unlikely that such inhibition could be connected with the suppression of acetylcholinesterase activity. Alternatively, a previous report showed the ability of the active ingredients in GL to modify the cAMP signaling [52]. However, GTs-mediated inhibition of $I_h$ in $GH_3$ cells could not be reversed by further addition of SQ-22536 (10 μM), an inhibitor of adenylate cyclase, (data not shown), suggesting that such an inhibitory action is apparently unlinked to the GTs effectiveness in cAMP signaling.

There is growing evidence to show that inflammatory pain could be closely linked to the magnitude of $I_h$ expressed in peripheral sensory neurons [40]. GTs was also previously reported to exert analgesic actions [11,53], which could be possibly associated with its inhibition of $I_h$ in different types of sensory

neurons. It is also important to note that the $I_h$ was expressed either in urinary bladder, ureter and renal pacemaker tissue or in different types of tumor cells (e.g., lung carcinoma cells) [34,54–57]; at extent GTs-induced block of $I_h$ is linked to its antineoplastic actions or impairments in urine excretion remains to be imperatively evaluated.

In addition to the reduction of $I_h$ amplitude, the $\tau_{act}$ value for $I_h$ activation observed in $GH_3$ cells was virtually raised in the presence of GTs. Although the detailed mechanism of GTs actions on $I_h$ is largely unresolved, these triterpenoids are likely to have greater affinity to the open/inactivated state than to the resting state residing in HCN channels, thus leading to a clear modification in the amplitude and gating of $I_h$. Nonetheless, GTs-mediated inhibition of $I_h$ can account largely for its suppression in the firing of spontaneous APs as well as in the amplitude of sag potential induced by long-lasting hyperpolarizing current stimuli.

There are four mammalian subtypes (HCN1, HCN2, HCN3 and HCN4), which have been cloned to date [30,33,58]. It is possible that HCN2, HCN3 or mixed HCN2 + HCN3 channels are functionally expressed in $GH_3$ or other types of endocrine cells [31,33]. Due to the importance of $I_h$ (i.e., KCNx-encoded currents) in contributing to excitability and automaticity of electrically excitable cells [27–29,31,41], findings from this study could provide novel insights into electrophysiological and pharmacological properties of GTs and other structurally related triterpenoids. Indeed, under our current-clamp recordings, addition of GTs was found to reduce the firing frequency of APs as well as sag potentials recorded from $GH_3$ cells. The reduction of AP firing caused by GTs could be primarily explained by its clear modifications in the amplitude and gating of $I_h$. However, it is important to note that the inhibitory effects of GTs on $I_h$ seen in $GH_3$ or HL-1 cells tend to be not isoform-specific. To what extent GTs-mediated change in endocrine cells [59] is linked to its suppression of $I_h$ observed in $GH_3$ cells remains to be determined. Moreover, whether GTs-induced bradycardia or cardioprotective effect [11,13,15] is intimately linked to its inhibitory effect on the amplitude and gating of $I_h$ in heart cells also imperatively needs to be studied.

The present results demonstrated that in HL-1 atrial cardiomyocytes, the addition of GTs was efficacious at suppressing $I_h$ elicited by a downsloping ramp pulse. A leftward shift in the steady-state activation curve of $I_h$ in $GH_3$ cells was demonstrated in its presence. Notably, recent reports have shown the ability of ivabradine, an inhibitor of $I_h$, to exert beneficial effects on post-resuscitation myocardial dysfunction [11,13,15,18,60]. It is thus tempting to anticipate that GTs-mediated inhibition of $I_h$ in heart cells could be closely linked to its beneficial effect on cardiac function.

## 3. Materials and Methods

### *3.1. Chemicals, Drugs and Solutions*

Adenosine deaminase, atropine, oxaliplatin and 8-(*p*-sulfophenyl)theophylline (8-PST) were obtained from Sigma-Aldrich (St. Louis, MO, USA), and 8-cyclopentyl-1,3-dipropylxanthine (DPCPX), SQ-22536, and zatebradine were from Tocris Cookson Ltd. (Bristol, UK), and carboxiplatin was from Pfizer (New Taipei City, Taiwan). *Ganoderma* triterpenoids (GTs) was kindly provided by Dr. Fan-E Mo, Department of Cell Biology and Anatomy, College of Medicine, National Cheng Kung University, Tainan, Taiwan, while chlorotoxin was by Dr. Woei-Jer Chuang, Department of Biochemistry, College of Medicine, National Chung Kung University, Tainan, Taiwan). GTs was dissolved in dimethyl sulfoxide (less than 0.01%) and made immediately prior to experiments. Unless stated otherwise, tissue culture media, horse serum, fetal bovine or calf serum, L-glutamine and trypsin/EDTA were acquired from Invitrogen (Carlsbad, CA, USA), while all other chemicals, such as CsCl, HEPES and aspartic acid, were of the best available quality, mostly at analytical grades.

The normal Tyrode's solution used in this study contained (in mM): NaCl 136.5, KCl 5.4, $CaCl_2$ 1.8, $MgCl_2$, 0.53, glucose 5.5 and HEPES-NaOH buffer 5.5 (pH 7.4). In whole-cell clamp experiments of recording membrane potential or $I_h$, we backfilled the pipette by using a solution (in mM): K-aspartate 130, KCl 20, $KH_2PO_4$ 1, $MgCl_2$, EGTA 0.1, $Na_2ATP$ 3, $Na_2GTP$ 0.1 and HEPES-KOH buffer 5 (pH 7.2).

The pipette solution and culture medium were commonly filtered on the day of use with Acrodisc® syringe filter with 0.2 μm Supor® membrane (Pall Corp., Port Washington, NY, USA).

### *3.2. Cell Preparations*

Pituitary tumor $GH_3$ cells, obtained from the Bioresources Collection and Research Center ((BCRC-60015); Hsinchu, Taiwan), were maintained in Ham's F-12 medium supplemented with 15% horse serum, 2.5% fetal calf serum and 2 mM L-glutamine, while the HL-1 atrial cell line was derived from the AT-1 mouse atrial cardiomyocyte tumor lineage, which was originally obtained from Louisiana State University in New Orleans, LA, USA. These cells were known to retain differentiated phenotypes of adult atrial myocytes [44,45]. Cells were maintained in Claycomb medium (Sigma-Aldrich) supplemented with 10% fetal bovine serum, 100 U/mL penicillin, 100 mg/mL streptomycin, 100 μM norepinephrine and 2 mM L-glutamine (Chang and Wu, 2018). $GH_3$ or HL-1 cells were grown in a humidified environment of 5% $CO_2$/95% air. In a separate set of experiments, HL-1 cells were treated with DPCPX (1 μM) at 37 °C for 6 h.

### *3.3. Electrophysiological Measurements*

Before the experiments, cells (i.e., $GH_3$ or HL-1 cells) were gently dispersed and a few drops of cell suspension were shortly transferred to a home-made chamber mounted on the fixed stage of inverted Diaphot-200 microscope (Nikon, Tokyo, Japan). They were immersed at room temperature (20–25 °C) in normal Tyrode's solution, the composition of which is described above. We fabricated the recording pipette from Kimax-51 capillary tubes (#34500; Kimble, Vineland, NJ, USA) using a vertical PP-83 puller (Narishige, Tokyo, Japan), and their tips were then fire-polished with MF-83 microforge (Narishige, Tokyo, Japan). During the measurements, the electrode with tip resistance of 3–5 MΩ, which was firmly inserted into holder, was maneuvered by use of WR-98 micromanipulator (Narishige, Tokyo, Japan). Patch-clamp experiments were measured in whole-cell arrangement (i.e., voltage- or current-clamp condition) by using an RK-400 patch-clamp amplifier (Bio-Logic, Claix, France) connected with an HP Pavilion X360 touchscreen laptop computer (14-cd1053TX; Hewlett-Packard, Palo Alto, CA, USA) [39,61]. Shortly before giga-seal formation was achieved, the potentials were corrected for the liquid junction potential that developed at the pipette tip, as the composition of pipette solution was different from that in the bath. The whole-cell results were corrected by the liquid junction potential measured under our experimental conditions (−12.5 ± 0.3 mV, $n$ = 14).

The dose-dependent relation of GTs on the inhibition of $I_h$ was least-squares fitted to the Hill equation by using nonlinear regression analysis (64-bit OriginPro 2016; Microcal, Northampton, MA). That is,

$$\text{Percentage inhibition} = (E_{max} \times \text{GTs}^{n_H}) / \left(\text{IC}_{50}^{n_H} + \text{GTs}^{n_H}\right),$$

where GTs represents the dose (μg/mL) of GTs; $IC_{50}$ and $n_H$ are the concentrations required for a 50% inhibition and the Hill coefficient, respectively and $E_{max}$ is GTs-induced maximal suppression of $I_h$.

To characterize the inhibitory action of GTs on $I_h$, the steady state activation curve of the current was constructed using a two-step protocol. The relationships between the conditioning potentials and the normalized amplitudes of $I_h$ with or without the addition of 10 μg/mL GTs were fitted with the goodness of fit by a Boltzmann function in the following form:

$$\frac{I}{I_{max}} = \frac{1}{1 + exp\left[\frac{\left(V - V_{\frac{1}{2}}\right)qF}{RT}\right]},$$

where $I_{max}$ is the maximal activated $I_h$; $V$ is the conditioning potential in mV; $V_{1/2}$ is the membrane potential (in mV) for half-maximal activation; $q$ is the apparent gating charge and $F$, $R$ or $T$ is Faraday's constant, the universal gas constant or the absolute temperature, respectively.

### *3.4. Statistical Analyses*

To perform linear or non-linear (e.g., sigmoidal or exponential function) curve fitting to the data set (i.e., the goodness of fit) was implemented by using either OriginPro 2016 (OriginLab, Northampton, MA, USA), pCLAMP 10.7 (Molecular Devices, San Jose, CA, USA) or Prism version 5.0 (GraphPad, La Jolla, CA, USA). Data were analyzed and are plotted using OriginPro (OriginLab), and they were expressed as mean ± standard error of the mean (SEM). The paired or unpaired Student's *t*-test, or one-way analysis of variance (ANOVA) followed by post-hoc Fisher's least-significance difference test for multiple comparisons, were implemented for the statistical evaluation of differences among means. We further used the non-parametric Kruskal–Wallis test, when the assumption of normality underlying ANOVA could be violated. Statistical analyses were performed by using IBM SPSS® version 20.0 (IBM Corp., Armonk, NY, USA). $p < 0.05$ was considered significant.

## 4. Conclusions

Although additional studies are needed to further validate our experimental results on different other types of cells, GTs-mediated inhibition of $I_h$ shown here could be an unidentified but the important ionic mechanism underlying the depressed excitability of $GH_3$ cells or HL-1 cardiomyocytes. However, these appreciable actions on $I_h$ presented herein are not explained solely by its possible binding to adenosine receptors.

**Author Contributions:** Conceptualization, S.-N.W.; methodology, S.-N.W.; investigation, W.-T.C., Z.-H.G., Y.-C.L., S.-N.W.; writing—original draft preparation, W.-T.C. and S.-N.W.; writing—review and editing, W.-T.C. and S.-N.W.; supervision, Y.-C.L., S.-N.W.; funding S.-N.W.

**Funding:** The research detailed in this paper is supported in part by grants awarded to S.-N. Wu which were provided both by National Cheng Kung University (D106-35A13, D107-F2519, D108-F2507 and NCKUH-10709001) from Ministry of Education, Taiwan, and by Ministry of Science and Technology (MOST-108-2314-B-006-094), Taiwan.

**Acknowledgments:** The authors would like to thank Kaisen Lee and Shih-Wei Li for contributing to part of the earlier experiments. Z.-H. Gao received a student fellowship from Ministry of Science and Technology, Taiwan, while S.-N. Wu received a Talent Award for the Outstanding Researchers from Ministry of Education, Taiwan.

**Conflicts of Interest:** The authors declare that there are no conflicts of interest.

## Abbreviations

| | |
|---|---|
| AP | action potential |
| DPCPX | 8-cyclopentyl-1,3-dipropylxanthine |
| GL | *Gandoderm lucidum* (Língzhī or Reishi) |
| GTs | *Ganoderma* triterpenoids |
| HCN gene | hyperpolarization-activated cyclic nucleotide-gated gene |
| *I-V* | current versus voltage |
| $IC_{50}$ | the concentration required for half-maximal inhibition |
| $I_h$ | hyperpolarization-activated cation current |
| 8-PST | 8-(*p*-sulfophenyl)theophylline |
| $\tau_{act}$ | activation time constant |

## References

1. Shiao, M.S. Natural products of the medicinal fungus *Ganoderma* lucidum: Occurrence, biological activities, and pharmacological functions. *Chem. Rec.* **2003**, *3*, 172–180. [CrossRef] [PubMed]
2. Chiu, H.F.; Fu, H.Y.; Lu, Y.Y.; Han, Y.C.; Shen, Y.C.; Venkatakrishnan, K.; Wang, C.K.; Golovinskaia, O. Triterpenoids and polysaccharide peptides-enriched *Ganoderma* lucidum: A randomized, double-blind placebo-controlled crossover study of its antioxidation and hepatoprotective efficacy in healthy volunteers. *Pharm. Biol.* **2017**, *55*, 1041–1046. [CrossRef] [PubMed]
3. Ahmad, M.F. *Ganoderma* lucidum: Persuasive biologically active constituents and their health endorsement. *Biomed. Pharmacother.* **2018**, *107*, 507–519. [CrossRef] [PubMed]

4. Cor, D.; Knez, Z.; Knez, H.M. Antitumour, Antimicrobial, Antioxidant and Antiacetylcholinesterase Effect of *Ganoderma* Lucidum Terpenoids and Polysaccharides: A Review. *Molecules* **2018**, *23*, 649. [CrossRef]
5. Xin, H.; Fang, L.; Xie, J.; Qi, W.; Niu, Y.; Yang, F.; Cai, D.; Zhang, Y.; Wen, Z. Identification and Quantification of Triterpenoids in Lingzhi or Reishi Medicinal Mushroom, *Ganoderma* lucidum (Agaricomycetes), with HPLC-MS/MS Methods. *Int. J. Med. Mushrooms* **2018**, *20*, 919–934. [CrossRef]
6. Liang, C.; Tian, D.; Liu, Y.; Li, H.; Zhu, J.; Li, M.; Xin, M.; Xia, J. Review of the molecular mechanisms of *Ganoderma* lucidum triterpenoids: Ganoderic acids A.; C2, D, F, DM, X and Y. *Eur. J. Med. Chem.* **2019**, *174*, 130–141. [CrossRef]
7. Peng, X.; Li, L.; Dong, J.; Lu, S.; Lu, J.; Li, X.; Zhou, L.; Qiu, M. Lanostane-type triterpenoids from the fruiting bodies of *Ganoderma* applanatum. *Phytochemistry* **2019**, *157*, 103–110. [CrossRef]
8. Kuok, Q.Y.; Yeh, C.Y.; Su, B.C.; Hsu, P.L.; Ni, H.; Liu, M.Y.; Mo, F.E. The triterpenoids of *Ganoderma* tsugae prevent stress-induced myocardial injury in mice. *Mol. Nutr. Food Res.* **2013**, *57*, 1892–1896.
9. Ma, B.; Ren, W.; Zhou, Y.; Ma, J.; Ruan, Y.; Wem, C.N. Triterpenoids from the spores of *Ganoderma* lucidum. *N. Am. J. Med. Sci.* **2011**, *3*, 495–498. [CrossRef]
10. Zhang, X.Q.; Ip, F.C.; Zhang, D.M.; Chen, L.X.; Zhang, W.; Li, Y.L.; Ip, N.Y.; Ye, W.C. Triterpenoids with neurotrophic activity from *Ganoderma* lucidum. *Nat. Prod. Res.* **2011**, *25*, 1607–1613. [CrossRef]
11. Chu, T.T.; Benzie, I.F.; Lam, C.W.; Fok, B.S.; Lee, K.K.; Tomlinson, B. Study of potential cardioprotective effects of *Ganoderma* lucidum (Lingzhi): Results of a controlled human intervention trial. *Br. J. Nutr.* **2012**, *107*, 1017–1027. [CrossRef] [PubMed]
12. Zhou, Y.; Qu, Z.Q.; Zeng, Y.S.; Lin, Y.K.; Li, Y.; Chung, P.; Wong, R.; Hägg, U. Neuroprotective effect of preadministration with *Ganoderma* lucidum spore on rat hippocampus. *Exp. Toxicol. Pathol.* **2012**, *64*, 673–680. [CrossRef] [PubMed]
13. Sudheesh, N.P.; Ajith, T.A.; Janardhanan, K.K. *Ganoderma* lucidum ameliorate mitochondrial damage in isoproterenol-induced myocardial infarction in rats by enhancing the activities of TCA cycle enzymes and respiratory chain complexes. *Int. J. Cardiol.* **2013**, *165*, 117–125. [CrossRef] [PubMed]
14. Wu, J.G.; Kan, Y.J.; Wu, Y.B.; Yi, J.; Chen, T.Q.; Wu, J.Z. Hepatoprotective effect of ganoderma triterpenoids against oxidative damage induced by tert-butyl hydroperoxide in human hepatic HepG2 cells. *Pharm. Biol.* **2016**, *54*, 919–929. [CrossRef] [PubMed]
15. Kirar, V.; Nehra, S.; Mishra, J.; Rakhee, R.; Saraswat, D.; Misra, K. Lingzhi or Reishi Medicinal Mushroom, *Ganoderma* lucidum (Agaricomycetes), as a Cardioprotectant in an Oxygen-Deficient Environment. *Int. J. Med. Mushrooms.* **2017**, *19*, 1009–1021. [CrossRef] [PubMed]
16. Chen, H.; Zhang, J.; Ren, J.; Wang, W.; Xiong, W.; Zhang, Y.; Bao, L.; Liu, H. Triterpenes and Meroterpenes with Neuroprotective Effects from *Ganoderma* leucocontextum. *Chem, Biodivers.* **2018**, *15*, e1700567. [CrossRef]
17. Hsu, P.L.; Lin, Y.C.; Ni, H.; Mo, F.E. *Ganoderma* Triterpenoids Exert Antiatherogenic Effects in Mice by Alleviating Disturbed Flow-Induced Oxidative Stress and Inflammation. *Oxid. Med. Cell. Longev.* **2018**, *2018*, 3491703. [CrossRef]
18. Veena, R.K.; Ajith, T.A.; Janardhanan, K.K. Lingzhi or Reishi Medicinal Mushroom, *Ganoderma* lucidum (Agaricomycetes), Prevents Doxorubicin-Induced Cardiotoxicity in Rats. *Int. J. Med. Mushrooms* **2018**, *20*, 761–774. [CrossRef]
19. Li, T.; Yu, H.; Song, Y.; Zhang, R.; Ge, M. Protective effects of *Ganoderma* triterpenoids on cadmium-induced oxidative stress and inflammatory injury in chicken livers. *J. Trace Elem. Med. Biol.* **2019**, *52*, 118–125. [CrossRef]
20. Liu, Y.N.; Tong, T.; Zhang, R.R.; Liu, L.M.; Shi, M.L.; Ma, Y.C.; Liu, G.Q. Interdependent nitric oxide and hydrogen peroxide independently regulate the coix seed oil-induced triterpene acid accumulation in *Ganoderma* lingzhi. *Mycologia* **2019**, *111*, 529–540. [CrossRef]
21. Lou, H.W.; Guo, X.Y.; Zhang, X.C.; Guo, L.Q.; Lin, J.F. Optimization of Cultivation Conditions of Lingzhi or Reishi Medicinal Mushroom, *Ganoderma* lucidum (Agaricomycetes) for the Highest Antioxidant Activity and Antioxidant Content. *Int. J. Med. Mushrooms* **2019**, *21*, 353–366. [CrossRef] [PubMed]
22. Wu, Y.; Han, F.; Luan, S.; Ai, R.; Zhang, P.; Li, H.; Chen, L. Triterpenoids from *Ganoderma* lucidum and Their Potential Anti-inflammatory Effects. *J. Agric. Food Chem.* **2019**, *67*, 5147–5158. [CrossRef] [PubMed]
23. Zhao, C.; Fan, J.; Liu, Y.; Guo, W.; Cao, H.; Xiao, J.; Wang, Y.; Liu, B. Hepatoprotective activity of *Ganoderma* lucidum triterpenoids in alcohol-induced liver injury in mice, an iTRAQ-based proteomic analysis. *Food Chem.* **2019**, *271*, 148–156. [CrossRef] [PubMed]

24. Socala, K.; Nieoczym, D.; Grzywnowicz, K.; Stefaniuk, D.; Wlaz, P. Evaluation of Anticonvulsant, Antidepressant-, and Anxiolytic-like Effects of an Aqueous Extract from Cultured Mycelia of the Lingzhi or Reishi Medicinal Mushroom *Ganoderma* lucidum (Higher Basidiomycetes) in Mice. *Int. J. Med. Mushrooms* **2015**, *17*, 209–218. [CrossRef]
25. Feng, X.; Wang, Y. Anti-inflammatory, anti-nociceptive and sedative-hypnotic activities of lucidone D extracted from *Ganoderma* lucidum. *Cell Mol. Biol.* **2019**, *65*, 37–42. [CrossRef]
26. Belardinelli, L.; Giles, W.R.; West, A. Ionic mechanisms of adenosine actions in pacemaker cells from rabbit heart. *J Physiol* **1988**, *405*, 615–633. [CrossRef]
27. Irisawa, H.; Brown, H.F.; Giles, W. Cardiac pacemaking in the sinoatrial node. *Physiol. Rev.* **1993**, *73*, 197–227. [CrossRef]
28. DiFrancesco, D.; Borer, J.S. The funny current: Cellular basis for the control of heart rate. *Drugs* **2007**, *67*, 15–24. [CrossRef]
29. Liu, Y.C.; Wang, Y.J.; Wu, P.Y.; Wu, S.N. Tramadol-induced block of hyperpolarization-activated cation current in rat pituitary lactotrophs. *Naunyn. Schmiedebergs Arch. Pharmacol.* **2009**, *379*, 127–135. [CrossRef]
30. He, C.; Chen, F.; Li, B.; Hu, Z. Neurophysiology of HCN channels: From cellular functions to multiple regulations. *Prog. Neurobiol.* **2014**, *112*, 1–23. [CrossRef]
31. Stojilkovic, S.S.; Tabak, J.; Bertram, R. Ion channels and signaling in the pituitary gland. *Endocr. Rev.* **2010**, *31*, 845–915. [CrossRef] [PubMed]
32. Datunashvili, M.; Chaudhary, R.; Zobeiri, M.; Luttjohann, A.; Mergia, E.; Baumann, A.; Balfanz, S.; Budde, B.; van Luijtelaar, G.; Pape, H.C.; et al. Modulation of Hyperpolarization-Activated Inward Current and Thalamic Activity Modes by Different Cyclic Nucleotides. *Front. Cell Neurosci.* **2018**, *12*, 369. [CrossRef] [PubMed]
33. Spinelli, V.; Sartiani, L.; Mugelli, A.; Romanelli, M.N.; Cerbai, E. Hyperpolarization-activated cyclic-nucleotide-gated channels: Pathophysiological, developmental, and pharmacological insights into their function in cellular excitability. *Can. J. Physiol. Pharmacol.* **2018**, *96*, 977–984. [CrossRef] [PubMed]
34. Byczkowicz, N.; Eshra, A.; Montanaro, J.; Trevisiol, A.; Hirrlinger, J.; Kole, M.H.; Shigemoto, R.; Hallermann, S. *HCN* channel-mediated neuromodulation can control action potential velocity and fidelity in central axons. *Elife* **2019**, 8. [CrossRef]
35. Hao, X.M.; Xu, R.; Chen, A.Q.; Sun, F.J.; Wang, Y.; Liu, H.X.; Chen, H.; Xue, Y.; Chen, L. *Endogenous HCN Channels* Modulate the Firing Activity of Globus Pallidus Neurons in Parkinsonian Animals. *Front. Aging Neurosci.* **2019**, *11*, 190. [CrossRef]
36. Romanelli, M.N.; Cerbai, E.; Dei, S.; Guandalini, L.; Martelli, C.; Martini, E.; Scapecchi, S.; Teodori, E.; Mugelli, A. Design, synthesis and preliminary biological evaluation of zatebradine analogues as potential blockers of the hyperpolarization-activated current. *Bioorg. Med. Chem.* **2005**, *13*, 1211–1220. [CrossRef]
37. Zhou, Y.; Wang, J.; Meng, Z.; Zhou, S.; Peng, J.; Chen, S.; Wang, Q.; Sun, K. Pharmacology of ivabradine and the effect on chronic heart failure. *Curr. Top Med. Chem.* **2019**. [CrossRef]
38. Hsiao, H.T.; Liu, Y.C.; Liu, P.Y.; Wu, S.N. Concerted suppression of Ih and activation of IK(M) by ivabradine, an HCN-channel inhibitor, in pituitary cells and hippocampal neurons. *Brain Res. Bull.* **2019**, *149*, 11–20. [CrossRef]
39. Wu, S.N.; Liu, S.I.; Hwang, T.L. Activation of muscarinic K+ channels by extracellular ATP and UTP in rat atrial myocytes. *J. Cardiovasc. Pharmaco.* **1998**, *31*, 203–211. [CrossRef]
40. Resta, F.; Micheli, L.; Laurino, A.; Spinelli, V.; Mello, T.; Mello, T.; Sartiani, L.; Di Cesare Mannelli, L.; Cerbai, E.; Ghelardini, C.; et al. Selective HCN1 block as a strategy to control oxaliplatin-induced neuropathy. *Neuropharmacology* **2018**, *131*, 403–413. [CrossRef]
41. Simasko, S.M.; Sankaranarayanan, S. Characterization of a hyperpolarization-activated cation current in rat pituitary cells. *Am. J. Physiol.* **1997**, *272*, E405–E414. [CrossRef] [PubMed]
42. Van Bogaert, P.P.; Pittoors, F. Use-dependent blockade of cardiac pacemaker current (If) by cilobradine and zatebradine. *Eur. J. Pharmacol.* **2003**, *478*, 161–171. [CrossRef] [PubMed]
43. Albertson, A.J.; Bohannon, A.S.; Hablitz, J.J. HCN Channel Modulation of Synaptic Integration in GABAergic Interneurons in Malformed Rat Neocortex. *Front. Cell Neurosci.* **2017**, *11*, 109. [CrossRef] [PubMed]
44. Claycomb, W.C.; Lanson, N.A.; Stallworth, B.S.; Egeland, D.B.; Delcarpio, J.B.; Delcarpio, J.B.; Bahinski, A.; Izzo, N.J., Jr. HL-1 cells: A cardiac muscle cell line that contracts and retains phenotypic characteristics of the adult cardiomyocyte. *Proc. Natl. Acad. Sci. USA* **1998**, *95*, 2979–2984. [CrossRef] [PubMed]

45. Chang, W.T.; Wu, S.N. Activation of voltage-gated sodium current and inhibition of erg-mediated potassium current caused by telmisartan, an antagonist of angiotensin II type-1 receptor, in HL-1 atrial cardiomyocytes. *Clin. Exp. Pharmacol. Physio.* **2018**, *45*, 797–807. [CrossRef] [PubMed]
46. Dongmo, A.B.; Azebaze, A.G.; Donfack, F.M.; Dimo, T.; Nkeng-Efouet, P.A.; Devkota, K.P.; Sontia, B.; Wagner, H.; Sewald, N.; Vierling, W. Pentacyclic triterpenoids and ceramide mediate the vasorelaxant activity of Vitex cienkowskii via involvement of NO/cGMP pathway in isolated rat aortic rings. *J. Ethnopharmacol.* **2011**, *133*, 204–212. [CrossRef]
47. Wei, J.C.; Wang, A.H.; Wei, Y.L.; Huo, X.K.; Tian, X.G.; Feng, L.; Ma, X.C.; Wang, C.; Huang, S.S.; Jia, J.M. Chemical characteristics of the fungus *Ganoderma* lucidum and their inhibitory effects on acetylcholinesterase. *J. Asian Nat. Prod. Res.* **2018**, *20*, 992–1001. [CrossRef]
48. Cheung, H.Y.; Ng, C.W.; Hood, D.J. Identification and quantification of base and nucleoside markers in extracts of *Ganoderma* lucidum, *Ganoderma* japonicum and *Ganoderma* capsules by micellar electrokinetic chromatography. *J. Chromatogr. A* **2001**, *911*, 119–126. [CrossRef]
49. Gao, J.L.; Leung, K.S.; Wang, Y.T.; Lai, C.M.; Li, S.P.; Hu, L.F.; Lu, G.H.; Jiang, Z.H.; Yu, Z.L. Qualitative and quantitative analyses of nucleosides and nucleobases in *Ganoderma* spp. by HPLC-DAD-MS. *J. Pharm. Biomed. Anal.* **2007**, *44*, 807–811. [CrossRef]
50. Khan, M.S.; Parveen, R.; Mishra, K.; Tulsawani, R.; Ahmad, S. Determination of nucleosides in Cordyceps sinensis and *Ganoderma* lucidum by high performance liquid chromatography method. *J. Pharm. Bioallied. Sci.* **2015**, *7*, 264–266.
51. Zaza, A.; Rocchetti, M.; DiFrancesco, D. Modulation of the hyperpolarization-activated current ($I_f$) by adenosine in rabbit sinoatrial myocytes. *Circulation* **1996**, *94*, 734–741. [CrossRef] [PubMed]
52. You, B.J.; Tien, N.; Lee, M.H.; Bao, B.Y.; Wu, Y.S.; Hu, T.C.; Lee, H.Z. Induction of apoptosis and ganoderic acid biosynthesis by cAMP signaling in *Ganoderma* lucidum. *Sci. Rep.* **2017**, *7*, 318. [CrossRef] [PubMed]
53. Collado Mateo, D.; Pazzi, F.; Dominguez Munoz, F.J.; Martin Martinez, J.P.; Olivares, P.R.; Gusi, N.; Adsuar, J.C. *Ganoderma* Lucidum Improves Physical Fitness in Women with Fibromyalgia. *Nutr. Hosp.* **2015**, *32*, 2126–2135. [PubMed]
54. Norberg, E.; Karlsson, M.; Korenovska, O.; Szydlowski, S.; Silberberg, G.; Uhlén, P.; Orrenius, S.; Zhivotovsky, B. Critical role for hyperpolarization-activated cyclic nucleotide-gated channel 2 in the AIF-mediated apoptosis. *EMBO J.* **2010**, *29*, 3869–3878. [CrossRef]
55. Hurtado, R.; Smith, C.S. Hyperpolarization-activated cation and T-type calcium ion channel expression in porcine and human renal pacemaker tissues. *J. Anat.* **2016**, *228*, 812–825. [CrossRef]
56. He, F.; Yang, Z.; Dong, X.; Fang, Z.; Liu, Q.; Hu, X.; Yu, S.; Li, L. The role of HCN channels in peristaltic dysfunction in human ureteral tuberculosis. *Int. Urol. Nephrol.* **2018**, *50*, 639–645. [CrossRef]
57. Mader, F.; Muller, S.; Krause, L.; Springer, A.; Kernig, K.; Protzel, C.; Porath, K.; Rackow, S.; Wittstock, T.; Frank, M.; et al. Hyperpolarization-Activated Cyclic Nucleotide-Gated Non-selective (HCN) Ion Channels Regulate Human and Murine Urinary Bladder Contractility. *Front. Physiol.* **2018**, *9*, 753. [CrossRef]
58. Furst, O.; D'Avanzo, N. Isoform dependent regulation of human HCN channels by cholesterol. *Sci. Rep.* **2015**, *5*, 14270. [CrossRef]
59. He, Y.M.; Zhang, Q.; Zheng, M.; Fan, Z.H.; Li, Y.H.; Zhang, D.; Zhang, Z.; Yuan, S.S.; Wang, Y.Y.; Zhou, P.; et al. Protective effects of a G. lucidum proteoglycan on INS-1 cells against IAPP-induced apoptosis via attenuating endoplasmic reticulum stress and modulating CHOP/JNK pathways. *Int. J. Biol. Macromol.* **2018**, *106*, 893–900. [CrossRef]
60. Kim, H.B.; Hong, Y.J.; Park, H.J.; Ahn, Y.; Jeong, M.H. Effects of Ivabradine on Left Ventricular Systolic Function and Cardiac Fibrosis in Rat Myocardial Ischemia-Reperfusion Model. *Chonnam. Med. J.* **2018**, *54*, 167–172. [CrossRef]
61. Huang, M.H.; Liu, P.Y.; Wu, S.N. Characterization of Perturbing Actions by Verteporfin, a Benzoporphyrin Photosensitizer, on Membrane Ionic Currents. *Front. Chem.* **2019**, *7*, 566. [CrossRef] [PubMed]


**Sample Availability:** Samples of the compounds are available from the authors upon requests.